DEVELOPMENT OF AN ANALYSIS TOOL FOR THE DESIGN OF BONDED COMPOSITE REPAIRS

Ralf J.C. Creemers

National Aerospace Laboratory NLR
Box 153, 8300 AD Emmeloord, The Netherlands
creemers@nlr.nl

ABSTRACT

Recent aircraft, both civil and military, show an increased use of composite materials in primary structures. Therefore, the Dutch Defence Materiel Organisation expressed the need for a design and analysis tool for bonded structural repairs. In the current paper, an Excel-based tool is presented which allows the specification of a wide variety of joint designs, including external patches, scarf repairs or a combination of the two. Adhesive plasticity and geometrically non-linear behaviour of the joint are taken into account. Still, analysis results are obtained rapidly, which is essential for use in the design process when the effects of different repair geometries are studied.

The design tool uses a discretised procedure for beam elongation and deflection in combination with an iterative numerical solution procedure. It was shown that the mathematical model of the discretised elements had to be modified slightly from the models currently used in literature in order to cope with repairs with small bending stiffness at their tips (tapered patch or thin first ply in a stepped design).

1. INTRODUCTION

With the increasing application of composite materials in primary structures of the near-future Royal Netherlands Air Force fleet, the number of damage occurrences and repairs is expected to increase as well. Damages falling within the limits posed by the Original Equipment Manufacturer (OEM) can be repaired following the guidelines of the Structural Repair Manual. A repair station may also repair damages exceeding these limits, but only after submittal to and approval by the OEM or cognisant engineering authority [1]. Analytical methods have to be available to substantiate the designed repair, and need to be supported by an experimentally verified database.

The Dutch Defence Materiel Organisation initiated a research programme to develop methods and procedures for inspection and repair of composite structures. One of the objectives of the programme is to develop a design and analysis tool for bonded composite repairs.

2. REPAIR DESIGN TOOL

2.1 General lay-out and capabilities

The developed repair design tool runs on a normal PC under Microsoft Office Excel, which is easily accessible for most people. For use in the design, the analysis of different repair configurations must be sufficiently simple and fast. Therefore, the 3D repair patch geometry is reduced to a 2D analysis of the joint cross-section, which should be sufficiently accurate for the purpose of designing repairs [2].

In the past, numerous theoretical analyses have been performed on bonded joints that determine adhesive shear and peel stresses. The classical models are the elastic solution by Volkersen [3] for double lap joints, and Goland and Reissner [4] for single lap joints. These solutions are extended by Hart-Smith [5] to cover adhesive plasticity, adherend stiffness imbalance and adherend thermal mismatch. However, in order to obtain explicit solutions the joint designs have always been somewhat limited. The

current design tool does not make use of the explicit solution, but uses a discretised procedure for beam elongation and deflection, in which the adhesive and both adherends are divided in a discrete number of elements. It has the advantage that each of these elements can have its own properties in terms of thickness, geometry, in-plane stiffness and bending stiffness. This presents a great variation in joint designs, including external patches and scarf repairs, specified via a simple-to-use and intuitive input interface that can be employed with only a minimum of training.
The user has to start with the definition of one or more adherend materials. Next, the joint geometry has to be specified, which is presented on-screen and changes real-time with the specification. The following geometrical options are available:

- Single/Double lap joint;
- Continuous/Ending base adherend;
- Multiple ply definition for base adherend;
- Multiple ply definition for the repair patch;
- Each ply in the repair can be defined as Stepped/Tapered;
- Each ply in the repair can be identified as part of a Patch/Scarf.

The base adherend is composed of any number of plies, each ply with its own material, thickness and orientation. Classical Laminate Theory is used to determine the resulting stiffness properties of the adherend. The base adherend is “Continuous” when at least some of the material runs from one side of the joint to the other; it is “Ending” when all of the adherend material is gradually run down or stopped abruptly. The repair patch may be composed of multiple plies or steps as well. When the repair ply is identified as “Patch” the ply is added externally; when identified as “Scarf” the ply replaces an equal amount of thickness in the base adherend. In both cases, each individual repair ply can be “Tapered” or “Stepped”. This enables the analysis of both tapered and stepped scarf repairs, possibly combined with an external (tapered or stepped) patch, see Figure 1.

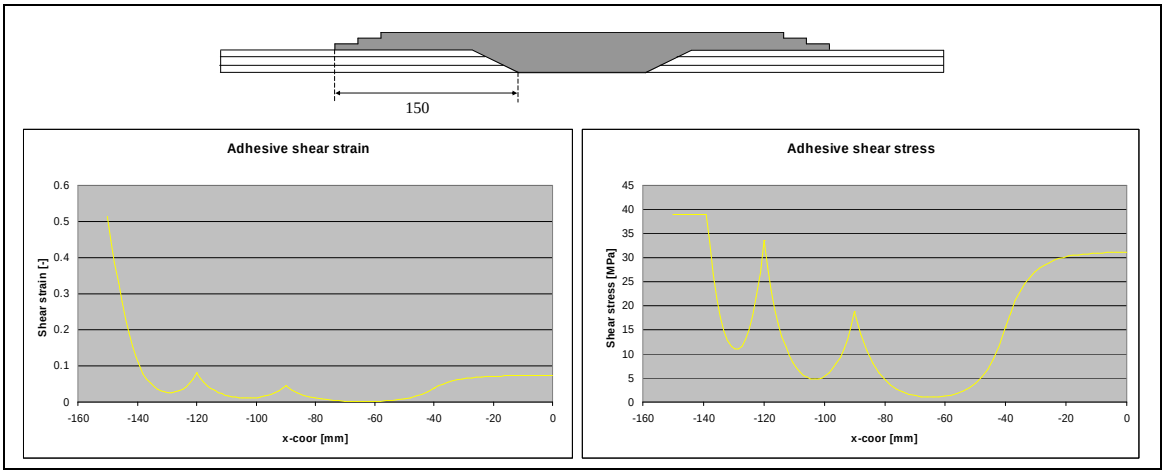

Figure 1: Shear strains and stresses in the adhesive including plasticity at the tip.

The following analysis results are generated and presented in the form of figures/tables:

- Adhesive shear strains and stresses including plastic behaviour (Figure 1);
- Adhesive peel stresses;
- Adherend loads (normal, transverse, bending);
- Adherend strains (mid-plane, curvature) and out-of-plane displacements.

Although adhesive plasticity and the geometrically non-linear behaviour of the joint (due to the repair patch eccentricity) are included in the analysis, results are obtained rapidly on a normal desktop PC.

2.2 Analysis procedure

Before discussing into more detail the discretised formulation of the joint and its numerical solution, Figure 2 shows the analysis procedure on its highest level. The analysis starts with adhesive shear strain and stress determination. No lateral deflections are included in the analysis, which effectively results in the Volkersen Shear Lag Equation [3] that is actually more appropriate for double than single lap joints. Next, the first peel stress analysis is performed, for which of course the lateral deflections of both adherends need to be calculated. The geometrically non-linear behaviour is already included here. Still, in case of significant bending strains, another analysis loop has to follow.

In the first analysis step, the adhesive shear strains are based on the adherend strains in the mid-plane (no bending). However, bending clearly influences the strains at the outside of the adherend, and by that the shear strains in the adhesive. These in turn influence the lateral deflections and peel stresses again. Usually convergence is reached quickly, as the effect of shear stresses on the lateral deflections and peel stresses is small compared to the contributions caused by geometrical eccentricities. Conversely, when the eccentricities themselves are small, little bending will occur and shear and peel stresses are already accurate.

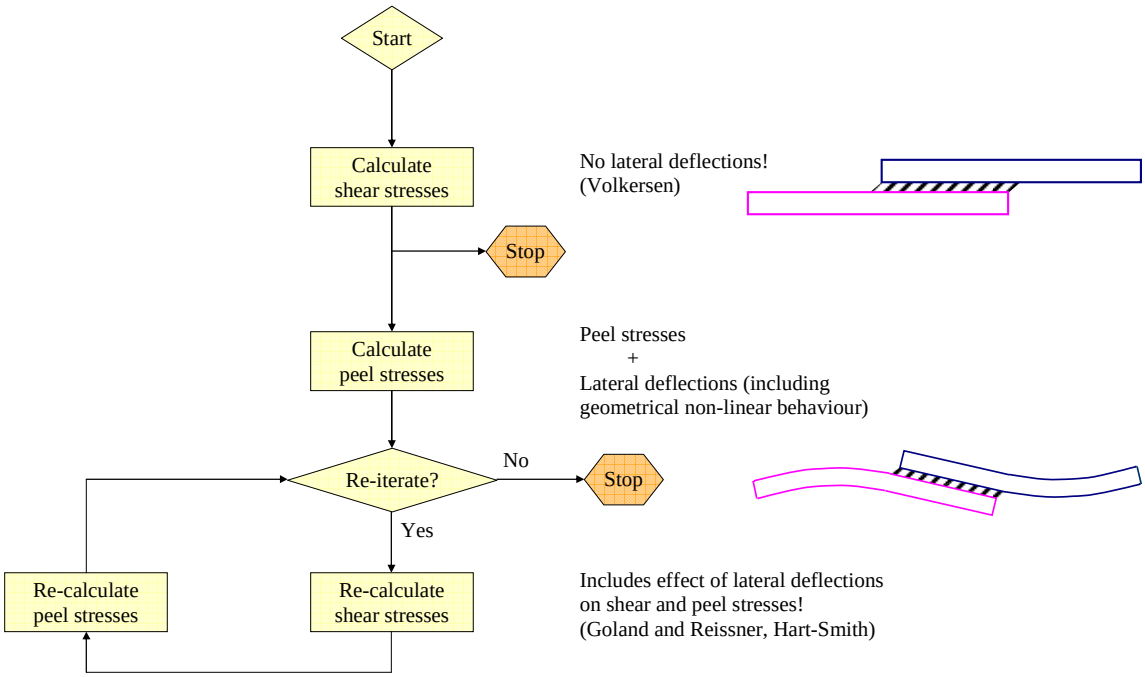

Figure 2: Analysis procedure of the Excel design tool.

Similar to Hart-Smith [5] the joint is divided in four sections (Figure 3) in the shear and peel stress analysis. For the deformations of sections C and D the analytical solution is available according to the classical theory for infinitesimal bending of thin plates:

$$T > 0 : w(x) = -\frac{M_0}{T} \cdot \cosh \lambda x + \frac{1}{\lambda} \cdot \left(w'_0 - \frac{V}{T} \right) \cdot \sinh \lambda x + \frac{V}{T} \cdot x + \frac{M_0}{T} + w_0, \lambda = \sqrt{\frac{T}{D}}$$
$$T < 0 : w(x) = -\frac{M_0}{T} \cdot \cos \lambda x + \frac{1}{\lambda} \cdot \left(w'_0 - \frac{V}{T} \right) \cdot \sin \lambda x + \frac{V}{T} \cdot x + \frac{M_0}{T} + w_0, \lambda = \sqrt{-\frac{T}{D}} \quad (1)$$

Geometrically non-linear behaviour is included. Different solutions have to be applied for tension and compression.

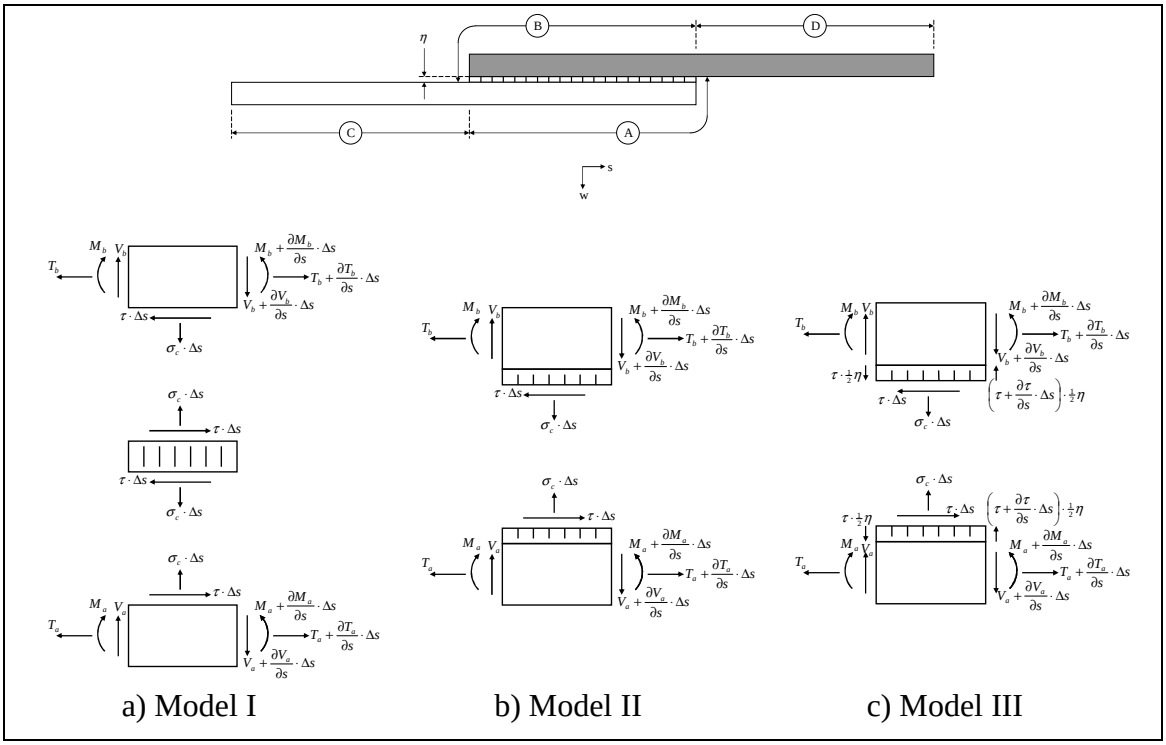

Figure 3: Mathematical models for analysis of lap joints.

For the deformations of sections A and B, the equations for force and moment equilibrium have to be set up based on a Free Body Diagram or mathematical model of the two adherends and adhesive, see Figure 3 and the next paragraph. Hart-Smith a.o. uses these equations to obtain an analytical solution for the deformation of both adherends, and from that deducts shear and peel stresses. In the current tool, however, each discretised element with length Δs is represented by a single row in Excel. By setting up the equations for force and moment equilibrium, the loads and deformations of one element can be predicted based on the loads and deformations of the previous element. When this is done for the entire joint from left to right, the loads (T, V, M) and deformations (δ, w, w') of all elements in sections A and B are known based on the loads and deformations of the first element. Geometrically non-linear behaviour is included in the equations for these discrete elements with length Δs.

The equations for the four sections can be arranged such that in total four (yet unknown) variables have to be determined to describe the behaviour of the entire joint:

- w_a' for the first element at the left side of section A;
- δ_b, w_b and w_b' for the first element at the left side of section B.

For double lap joint configurations this reduces to three variables, as $w_a' = 0$ for the entire joint. All other required input data is given by Eq. 1 and its derivatives, combined with the boundary conditions for section C (clamped or simply supported at the left) and section B (free left end).

Now, with arbitrary assumed values for these four variables, the loads and deformations at the right side of sections A and B can be calculated, while Eq. 1 gives the data for section D. Next, an iterative numerical solution procedure can be used to find the unique values for these variables that satisfy the boundary conditions at the right end of sections A (free) and D (clamped or simply supported).

The iterative numerical solution procedure that was implemented in Excel to solve for the unknown variables is called the Modified Simplex Method [6,7]. It is a “trial-and-

error" method, but more efficient than the non-systematic approaches or the one-variable-at-a-time method. Basically, in the simplex method the trial with the least favourable response value is reflected into the control variable space opposite the undesirable result. This leads to a new least favourable response value, which is to be reflected again, and so on. In the modified simplex method these moves are allowed to expand or contract, enabling the simplex both to accelerate along a successful track and home in on the optimum.
In the current Excel-tool the four variables are not determined all at the same time. Figure 2 shows that shear and peel stresses are determined separately through the separate analysis of in-plane deformations and out-of-plane deflections. It goes beyond the scope of this paper to explain into detail the reasons for this approach, but it relates to the numerical accuracy in Excel. It suffices to say that the approach allows the shear stress to be determined via δ_b, independently from the peel stress via w_a', w_b and w_b'.

In the shear stress analysis, adhesive plasticity is included. The actual shear stress-strain curve of an adhesive is approximated either by a perfectly plastic material or by a material that exhibits a bi-linear behaviour. Both methods are based on equivalent strain energy at final failure [8].
The bi-linear approximation allows adhesive plasticity to be included in the analyses without any increase of CPU-time. Several adhesives are pre-programmed (FM300, AF163), but one can also apply a user-defined adhesive.

2.3 Discretised formulation of the joint
Three different methods or mathematical models have been investigated for the discretisation of sections A and B into elements with length Δs, see Figure 3. The drawings are somewhat simplified (no out-of-plane deflections, or tapered/scarfed elements are drawn) in order to emphasize the differences between the models.
The first model in Figure 3 is used by Volkersen [3] and Hart-Smith [8] to determine shear stresses and peel stresses in double-lap joint configurations. At first glance, accurate results are also obtained for the single-lap joint configuration of Figure 4. However, detailed inspection of the displacements shows a discrepancy. For (high-enough) loads, the displacements should converge to $w = \frac{1}{2}\cdot(t_b + \eta) = 0.8325$ mm, while the analysis finds a displacement of only 0.75 mm. The difference is caused by neglecting the thickness of the adhesive layer (0.165 mm) in the equations of the bending moments. Further investigation shows that the global equilibrium of moments is not completely satisfied. A small contribution of in total $N\cdot\eta$ is missing.
The discrepancy is corrected by Hart-Smith in [5] by giving an offset of $\frac{1}{2}\eta$ to the adhesive shear stress components in the equations for the bending moments of the single-lap joint, which effectively results in the model shown in Figure 3b and the following basic equations:

$$\begin{array}{lll} \dfrac{\partial T_a}{\partial s} = -\tau & \dfrac{\partial V_a}{\partial s} = \sigma_c & \dfrac{\partial M_a}{\partial s} = V_a - T_a \cdot \dfrac{\partial w_a}{\partial s} + \tau \cdot \left(\dfrac{t_a + \eta}{2} \right) \\ \dfrac{\partial T_b}{\partial s} = \tau & \dfrac{\partial V_b}{\partial s} = -\sigma_c & \dfrac{\partial M_b}{\partial s} = V_b - T_b \cdot \dfrac{\partial w_b}{\partial s} + \tau \cdot \left(\dfrac{t_b + \eta}{2} \right) \end{array} \quad (2)$$

This indeed corrects the global moment equilibrium and the resulting out-of-plane displacements, see Figure 4b. However, locally, still a small error is introduced in the equations for the bending moments. Under normal circumstances this error is not likely to appear, but for the case of a tapered patch, the tip of the patch has such a small bending stiffness that any small error in the bending moment reveals itself in the

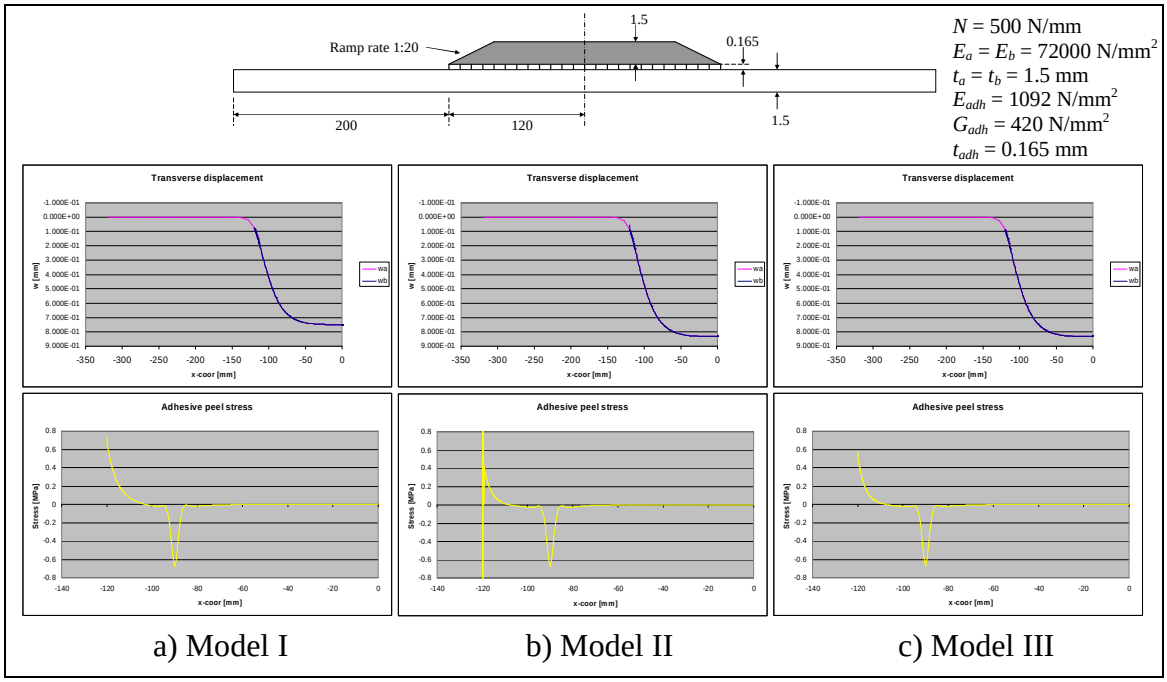

a) Model I b) Model II c) Model III

Figure 4: Analysis results for a tapered patch with three different mathematical models.

out-of-plane bending behaviour, which in turn results in deviant displacements and peel stresses at the tip, see Figure 4b. It is important to realise that this behaviour cannot be corrected by the application of finer elements at the tip; it is inherent to the chosen mathematical model.

In Figure 3c an alternative mathematical model for single-lap joints is proposed. It introduces a shear stress derivative in the equations for transverse force equilibrium:

$$\begin{aligned} \frac{\partial T_a}{\partial s} &= -\tau \quad ; \quad \frac{\partial V_a}{\partial s} = \sigma_c + \frac{\partial \tau}{\partial s}\cdot\tfrac{1}{2}\eta \quad ; \quad \frac{\partial M_a}{\partial s} = V_a - T_a\cdot\frac{\partial w_a}{\partial s} + \tau\cdot\tfrac{1}{2}t_a \\ \frac{\partial T_b}{\partial s} &= \tau \quad\quad \frac{\partial V_b}{\partial s} = -\sigma_c + \frac{\partial \tau}{\partial s}\cdot\tfrac{1}{2}\eta \quad\quad \frac{\partial M_b}{\partial s} = V_b - T_b\cdot\frac{\partial w_b}{\partial s} + \tau\cdot\tfrac{1}{2}t_a \end{aligned} \tag{3}$$

Global moment equilibrium is obtained through the transverse forces instead of an offset to the adhesive shear stress components. To also obtain global equilibrium for the transverse forces themselves, it is necessary now to increase the transverse force value at the start of section A with the shear stress component $\tau\cdot\eta$ at the start of the adhesive layer, and to decrease the transverse force value at the start of section D with the shear stress component $\tau\cdot\eta$ at the end of the adhesive layer.

This last model has been implemented in Excel, and it results in accurate displacements and correct peel stresses at the tip (Figure 4c). However, an analytical deduction of shear and peel stresses, as in [4,5] is much more complicated (if not impossible) for this model due to the shear stress derivatives in the transverse force equations.

3. VALIDATION

A numerical validation of the design tool has been performed based on data from literature and detailed Finite Element Analysis. Shear and peel stresses for a double lap and strap joint are given in Figure 6.2.3.4.1(b) of reference [1]. The stresses have been re-calculated with the current design tool and the results are shown in Figure 5. Comparison with [1] shows that both shear and peel stresses are exactly the same, which was to be expected because identical mathematical models (Model I) are applied for the double-lap joint configuration.

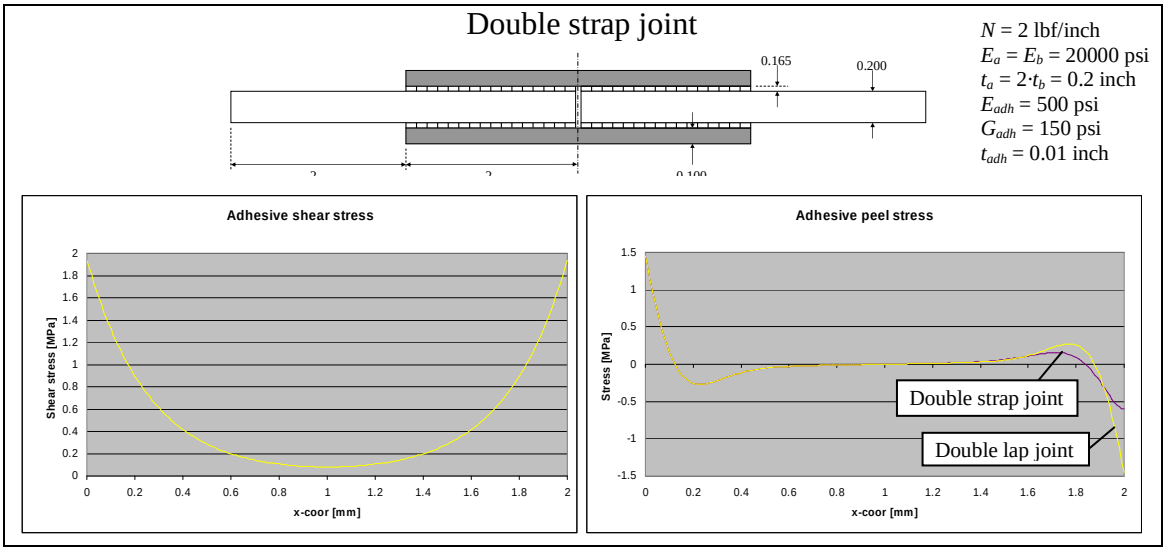

Figure 5: Shear and peel stresses in a double lap and strap joint.

However, for the single-lap joint an alternative mathematical model is used, i.e. Model III instead of II. It has already been shown that it gives better peel stress results for configurations with tip tapering. Although usually not as apparent as for the tapered design, dissimilarities are also found for stepped designs. Research showed, that the lower the bending stiffness at the tip, the larger the difference between the two models. Further, there is no theoretical limit to this divergence. Moreover, Model II always finds higher peel stresses than Model III due to the overestimated bending moment.
Several tests have been performed to check the (geometrically non-linear) behaviour of the Excel-tool with the selected mathematical Model III. An FE model of a single-lap joint was analysed with a very fine mesh at both ends of the bond layer. Stresses in the middle of the bond layer are compared to the Excel results. Due to the free edges of the bond layer, the FE analysis enforces the shear stresses to be zero at the beginning and the end. Apart from that, excellent agreement (within 1%) is found between FEM and the Excel-tool, also for the displacements, mid-plane strains and bending strains. For this particular joint, application of Model II finds peel stresses that are 10% too high.
As geometrically non-linear behaviour is included in all equations in the Excel-tool, application of a compressive load in combination with a thin external patch, which acts as an imperfection, should result in buckling. The buckling load for beams can be

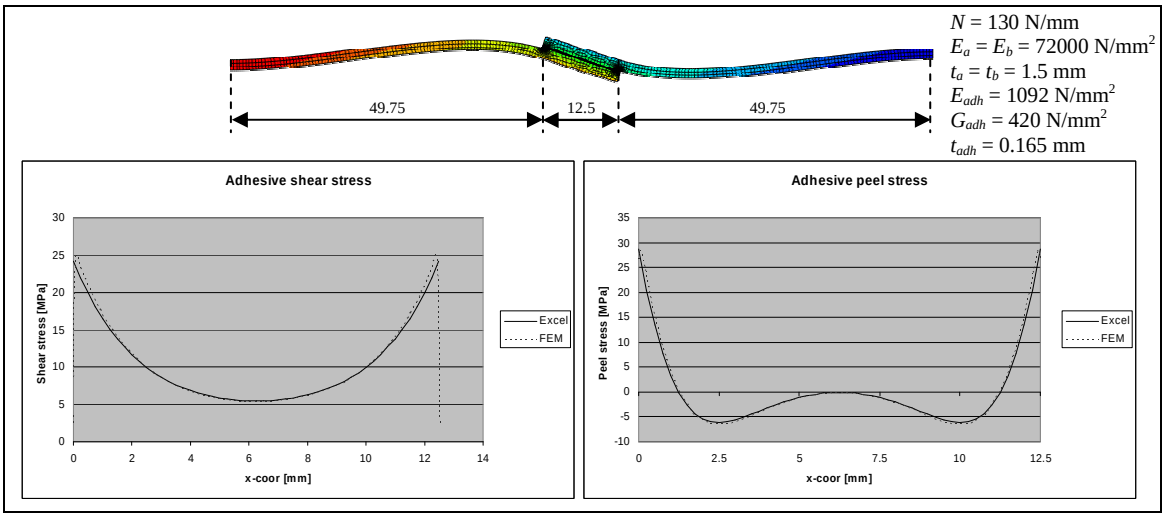

Figure 5: Shear and peel stresses in a double lap and strap joint.

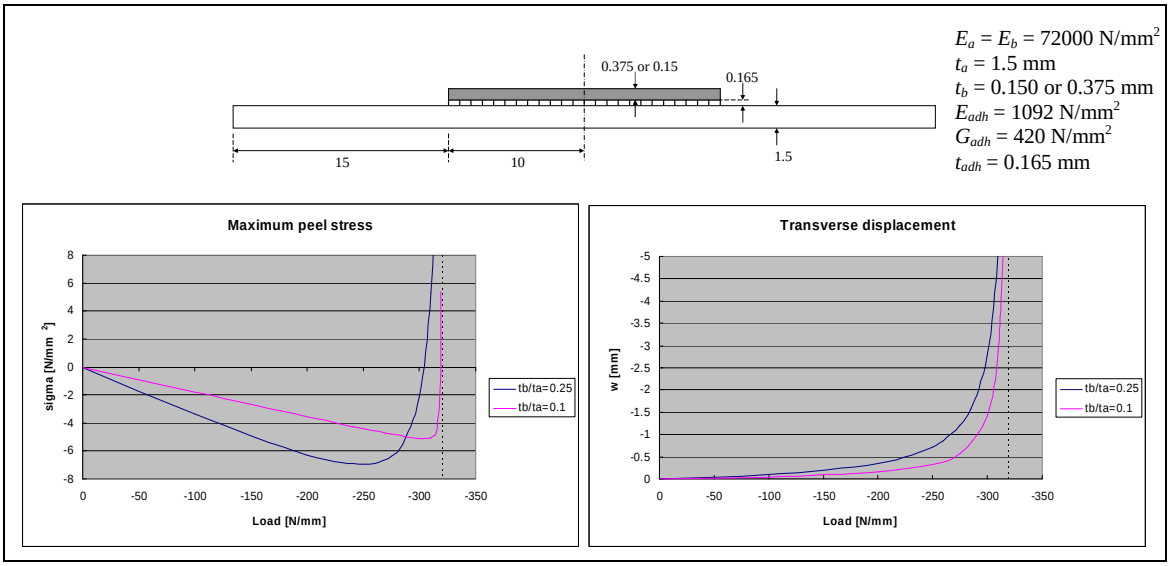

Figure 6: Peel stresses and transverse displacements at different load levels.

calculated with:

$$P_{Euler} = -k_b \cdot \frac{\pi^2 EI}{L^2} \tag{4}$$

For clamped boundary conditions k_b = 4. The analysis results for two different patch thicknesses are shown in Figure 6. As one would expect, displacements increase exponentionally for load levels approaching the theoretical buckling load.

Finally, the equations for a tapered scarf are validated. They differ fundamentally from the equations of a stepped scarf or patch, because adhesive shear and peel stresses are acting under an angle now. For a scarf joint consisting of two identical materials and with a constant scarf angle, shear and peel stresses in the adhesive are constant along the entire joint. Their values can be calculated with:

$$\tau = \frac{N}{t} \cdot \cos\theta \cdot \sin\theta \qquad \text{and} \qquad \sigma_c = \frac{N}{t} \cdot \sin^2\theta \tag{5}$$

For two different scarf ratios (1:20 and 1:10) the shear and peel stresses have been determined, see Figure 7. The Excel-tool indeed finds constant stresses and they agree exactly with the theoretical values of Eq. 5.

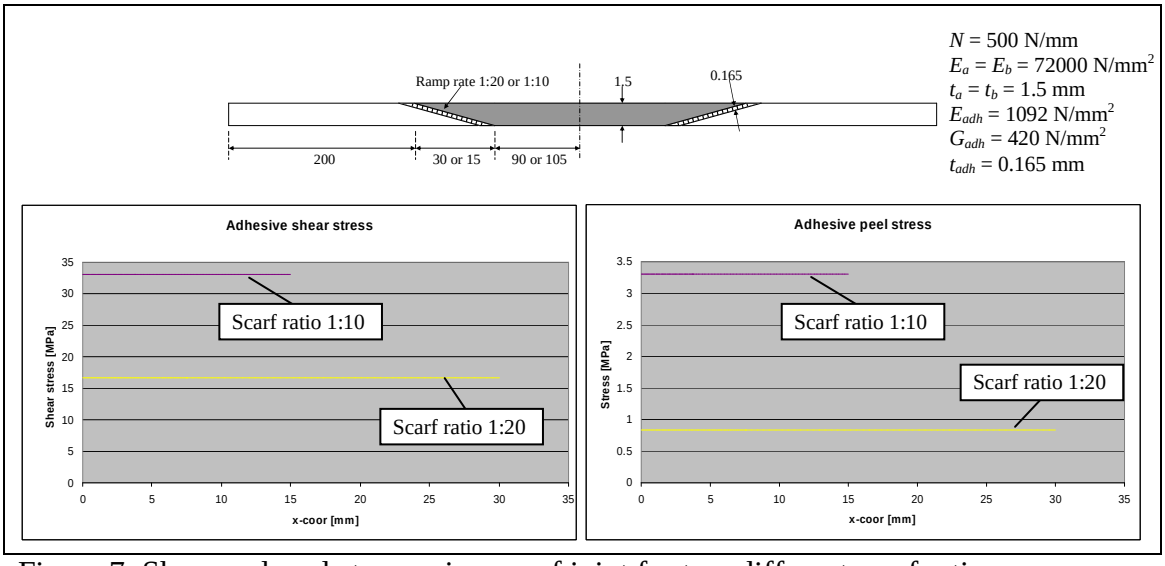

Figure 7: Shear and peel stresses in a scarf joint for two different scarf ratios.

4. STRESS DISTRIBUTION IN A COMPOSITE SCARF REPAIR

As an example, the design tool is used to investigate stresses in a tapered and stepped scarf joint for two laminates, both of 4 mm thickness and with a quasi-isotropic lay-up consisting of Cytec 977-2/HTA-12K-UD-Tape with the following ply properties:

E_1 = 124450 MPa G_{12} = 3900 MPa

E_2 = 7900 MPa ν_{12} = 0.28 MPa

The material is available in a variant with 0.125 mm ply thickness, and also in a "Thick tape" variant with ply thickness 0.250 mm. The first laminate is built up with 32 plies of 0.125 mm. The second laminate contains 16 plies of 0.250 mm:

- Lay-up 1: $[45/0/-45/90]_{4S}$ t_{ply} = 0.125 mm
- Lay-up 2: $[45/0/-45/90]_{2S}$ t_{ply} = 0.250 mm

Each ply that is removed from the base laminate is replaced by an identical ply with the same orientation. Figure 8 shows the user-input needed to specify the geometry of the stepped scarf joint. Please notice that in the stepped design, the first ply is placed on top of the base laminate ("Patch" instead of "Scarf") and the last ply is a filler ply.

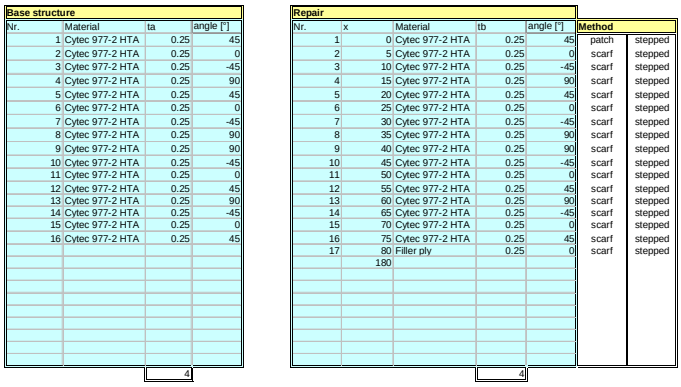

Base structure

Nr.	Material	ta	angle [°]
1	Cytec 977-2 HTA	0.25	45
2	Cytec 977-2 HTA	0.25	0
3	Cytec 977-2 HTA	0.25	-45
4	Cytec 977-2 HTA	0.25	90
5	Cytec 977-2 HTA	0.25	45
6	Cytec 977-2 HTA	0.25	0
7	Cytec 977-2 HTA	0.25	-45
8	Cytec 977-2 HTA	0.25	90
9	Cytec 977-2 HTA	0.25	90
10	Cytec 977-2 HTA	0.25	-45
11	Cytec 977-2 HTA	0.25	0
12	Cytec 977-2 HTA	0.25	45
13	Cytec 977-2 HTA	0.25	90
14	Cytec 977-2 HTA	0.25	-45
15	Cytec 977-2 HTA	0.25	0
16	Cytec 977-2 HTA	0.25	45

4

Repair

Nr.	x	Material	tb	angle [°]	Method	
1	0	Cytec 977-2 HTA	0.25	45	patch	stepped
2	5	Cytec 977-2 HTA	0.25	0	scarf	stepped
3	10	Cytec 977-2 HTA	0.25	-45	scarf	stepped
4	15	Cytec 977-2 HTA	0.25	90	scarf	stepped
5	20	Cytec 977-2 HTA	0.25	45	scarf	stepped
6	25	Cytec 977-2 HTA	0.25	0	scarf	stepped
7	30	Cytec 977-2 HTA	0.25	-45	scarf	stepped
8	35	Cytec 977-2 HTA	0.25	90	scarf	stepped
9	40	Cytec 977-2 HTA	0.25	90	scarf	stepped
10	45	Cytec 977-2 HTA	0.25	-45	scarf	stepped
11	50	Cytec 977-2 HTA	0.25	0	scarf	stepped
12	55	Cytec 977-2 HTA	0.25	45	scarf	stepped
13	60	Cytec 977-2 HTA	0.25	90	scarf	stepped
14	65	Cytec 977-2 HTA	0.25	-45	scarf	stepped
15	70	Cytec 977-2 HTA	0.25	0	scarf	stepped
16	75	Cytec 977-2 HTA	0.25	45	scarf	stepped
17	80	Filler ply	0.25	0	scarf	stepped
	180					

4

Figure 8: Specification of a 16 ply stepped scarf joint (ratio 1:20).

For the tapered scarf design adhesive shear and peel stresses will no longer be constant, as is the case for a real isotropic material (see Figure 7 once again). This is caused by the inhomogeneous nature of the laminate with the stiff 0-degree plies carrying the major part of the load. When this load has to be transferred by the bond layer, this results in an increase in shear and peel stresses. The phenomenon is the same for both lay-ups, see Figure 9. For Lay-up 1 eight peeks are found, because the laminate contains eight 0-degree plies, and it follows naturally that for Lay-up 2 four peeks are found. More or less the same behaviour is found for the stepped scarf design.

Lay-up 1 may contain more peeks than Lay-up 2, but the maximum shear and peel stress values are lower. This cannot be attributed to the smaller load stored in a thin ply compared to a thick ply because the length of the bond layer is smaller by the same factor; the amount of load per unit length of the bond layer is the same. The lower peeks are explained by the damping effect of the surrounding "soft" plies. These plies and their low stresses influence the stresses in the "stiff" ply. When the stiff ply is thin, stresses simply do not have the chance to reach their maximum value. For ultra-thick plies or very thick clusters, the peek stresses would actually go over to a plateau with constant (high) stress values. For the same reasons the minimum stresses are slightly lower for the lay-up with thick plies.

From Figure 9 it can be concluded that the more homogenous a laminate is through the thickness (many thin plies), the more constant the shear and peel stress are for a scarf repair. Therefore, from the point of view of the bond layer strength in a repair, it is beneficial to build a laminate with thin plies rather than heavy thick plies.

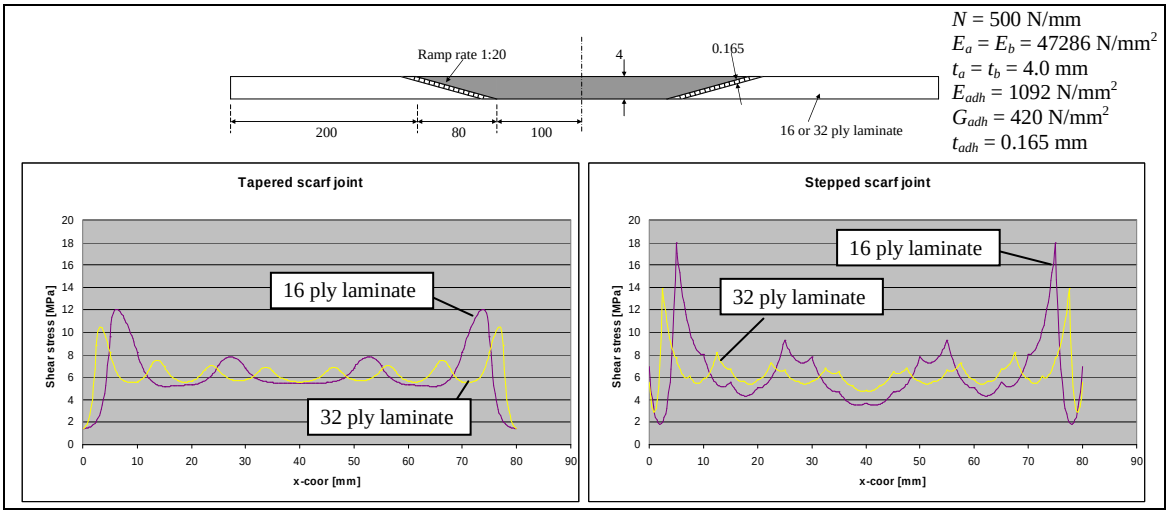

Figure 9: Shear stresses in a tapered and stepped scarf joint.

5. CONCLUSIONS

A repair design tool has been developed that runs under Microsoft Office Excel, making it easily accessible for most people. A wide variety of joint designs, including external patches and (tapered or stepped) scarf repairs, can be specified via a simple-to-use input interface that can be employed with only a minimum of training. Although adhesive plasticity and the geometrically non-linear behaviour of the joint are taken into account the analysis results are accurate and obtained rapidly, making the tool pre-eminently suitable for use in the design process.

It was shown that the mathematical model for single-lap joints used by Goland and Reissner in [4] and Hart-Smith in [5] should be modified in order to cope with designs that have small bending stiffness at the tip, such as tapered patches (but also stepped designs with a thin first ply). Accurate results are obtained with an alternative model that includes the adhesive shear stress derivative in the transverse force equations.

ACKNOWLEDGEMENTS

The work presented in this paper has been funded by the Dutch Ministry of Defence in the National Technology Programme “Inspection and repair techniques for composite structures” under contract number N04/27.

REFERENCES

1- “Composite materials handbook – Polymer matrix composites materials usage, design, and analysis”, *MIL-HDBK-17-3F*, 2002.
2- Wang, C.H., Gunnion, A., “Design Methodology for Scarf Repairs to Composite Structures”, *DSTO-RR-0317*, 2006.
3- Volkersen, O., “Die Nietkraftverteilung in Zugbeanspruchten Nietverbindungen mit konstanten Laschenquerschnitten”, *Luftfahrtforschung*, 1938;15:41-47.
4- Goland, M., Reissner, E., “The Stresses in Cemented Joints”, *Journal of Applied Mechanics*, 1944;11:A17-A27.
5- Hart-Smith, L.J., “Adhesive-bonded single-lap joints”, *NASA-CR-112236*, 1973.
6- Nelder, J.A., Mead, R., “A simplex method for function minimization”, *Computer Journal*, 1965;7:308-313.
7- Åberg, E.R., Gustavsson, A.G.T., “Design and evaluation of modified simplex methods”, *Analytica Chimica Acta*, 1982;144:39-53.
8- Hart-Smith, L.J., “Adhesive-bonded double-lap joints”, *NASA-CR-112235*, 1973.